Nuclear Engineering and Design 76 (1983) 137–151
North-Holland, Amsterdam

A STUDY OF DISPLACEMENT-BASED FLUID FINITE ELEMENTS FOR CALCULATING FREQUENCIES OF FLUID AND FLUID–STRUCTURE SYSTEMS

Lorraine G. OLSON and Klaus-Jürgen BATHE

Department of Mechanical Engineering, Massachusetts Institute of Technology, Cambridge, MA 02139, USA

Received May 1983

The widely-used displacement-based finite element formulation for inviscid, compressible, small displacement fluid motions is examined, with the specific objective of calculating fluid–structure frequencies. It is shown that the formulation can be employed with confidence to predict the static response of fluids. Also the resonant frequencies of fluids in rigid cavities and the frequencies of fluids in flexible boundaries are solved successfully if a penalty on rotations is included in the formulation. However, the reason for writing this paper is that problems involving structures moving through fluids that behave almost incompressibly – such as an ellipse vibrating on a spring in water – could not be solved satisfactorily, for which a general explanation is given.

1. Introduction

Fluid–structure interactions must be considered in the design of marine platforms, nuclear power plants, hydroelectric dams, and other structures. Therefore, significant efforts have gone into developing general purpose finite element techniques for modeling complex fluid–structure systems.

Most fluid–structure interaction analyses are based on simplifying assumptions (e.g. inviscid flow) which allow one of two approaches:

(1) Displacements are the variables in the solid, pressures (or velocity potentials) are the variables in the fluid.
(2) Displacements are the variables in both the fluid and the solid.

Zienkiewicz and Bettess [1] and Belytschko [2,3] survey work in both areas.

Various authors have employed the first approach, since it requires only one variable at each fluid finite element node. Zienkiewicz and Newton [4] and Craggs [5] detail typical formulations. However, existing formulations generally involve unsymmetric matrices (which can be made symmetric through secondary transformations) that render them difficult to incorporate in general finite element analysis programs [6,7,8].

For structural analysis the general finite element codes use a Lagrangian mesh to describe the displacements of solids. This makes a Lagrangian displacement-based fluid element very desirable. Existing program libraries for structural elements can readily incorporate displacement-based fluid elements because the final element matrices are symmetric and positive definite. In addition, the resulting matrices have relatively narrow bandwidths so that existing equation solution methods perform efficiently.

Several researchers have employed displacement-based fluid elements. Belytschko has used this approach extensively in linear and nonlinear transient fluid–structure interaction problems [9–13]. Bathe and Hahn [14] and Larsson and Svenkvist [15] also employed displacement-based fluid elements for transient analysis. Gladwell and Zimmerman [16] and Gladwell [17] present a variational formulation of acousto-structural problems using displacements or pressures as variables. Chopra, Wilson, and Farhoomand [18], Wilson [19], Shantaram et al. [20], Shugar and Katona [21], and Khalil and Hubbard [22] also use the displacement-based fluid model for transient analysis.

However, although various applications have been reported using displacement-based fluid elements, there are still some difficult questions to address regarding the applicability of the formulation to various analyses. As earlier noted by Kiefling and Feng [23], Akkas, Akay, and Yilmaz [24], and Hamdi, Ousset, and Verchery [25], the displacement-based fluid elements employed in practice can exhibit spurious oscillations. We address this specific problem in this paper. In the

next two sections we briefly review the formulation of the fluid finite element, and in section 4 we report on various sample analyses that we have conducted. The objective with these analyses was to gain insight into the behaviour and characteristics of the fluid element. The result of these investigations, summarized in section 5, is that the element can be employed for static analysis and prediction of fluid frequencies in cavities with rigid or flexible boundaries, but there are significant difficulties in using the element satisfactorily for analyses of structures moving through fluids.

A remark

With the material in this paper we do not advance the state-of-the-art by introducing a "new" formulation or procedure, instead we humbly report on our failure to solve what some reseachers may consider a rather simple problem with an otherwise powerful technique. In sections 2 through 4.3 we review the existing formulation to show that our program implementation performs well in several categories of standard analyses – merely to underline that we can solve certain problems with confidence. Then in section 4.4 we discuss the inability of the formulation to handle the important class of problems in which a structure vibrates in fluid that acts as almost incompressible. The contribution in this paper – we believe – lies in providing some important insight into a method quite widely employed for analysis.

2. Assumptions and governing equations

In deriving the governing differential equations for the fluid, we make the usual acoustic wave theory approximations. The fluid motion is assumed to be inviscid, compressible, and adiabatic. Body forces are neglected. Also, the fluid density is taken to be a function of pressure only (not temperature) so that the density is barotropic. Consequently, the fluid motion is both isentropic and irrotational.

With these simplifications, the momentum equation for the fluid becomes

$$\rho \frac{\partial^2 \boldsymbol{U}}{\partial t^2} = -\nabla p, \tag{1}$$

where ρ = fluid particle density, $\boldsymbol{U}$ = fluid particle displacement and p = pressure in fluid particle (positive for compression).

The continuity, energy, and constitutive relations combine to give,

$$p = -\beta(\nabla \cdot \boldsymbol{U}), \tag{2}$$

where β is the isentropic bulk modulus of fluid. If we present our differential equations in standard form in terms of velocity potentials, $\dot{\boldsymbol{U}} = \nabla\phi$, we find that

$$\beta \nabla^2 \phi = \rho \frac{\partial^2 \phi}{\partial t^2}. \tag{3}$$

For displacement-based finite element analysis we write this equation in the form

$$\beta \nabla(\nabla \cdot \boldsymbol{U}) = \rho \frac{\partial^2 \boldsymbol{U}}{\partial t^2}. \tag{4}$$

Note that since the fluid is inviscid, it can "slip" (move tangentially) along solid boundaries.

3. Finite element formulation

To establish a virtual work expression, we must consider the weak form of eq. (4)

$$\int_V \beta \nabla(\nabla \cdot \boldsymbol{U}) \cdot \delta \boldsymbol{U} \, \mathrm{d}V = \int_V \rho \frac{\partial^2 \boldsymbol{U}}{\partial t^2} \cdot \delta \boldsymbol{U} \, \mathrm{d}V, \tag{5}$$

where the right hand side is the standard d'Alembert force integral. In order to integrate the left hand side we make use of the vector identity

$$(\nabla a) \cdot \boldsymbol{w} = \nabla \cdot (a\boldsymbol{w}) - a(\nabla \cdot \boldsymbol{w}). \tag{6}$$

Let $\boldsymbol{w} = \delta \boldsymbol{U}$ and $a = \nabla \cdot \boldsymbol{U}$ in eq. (6) so that

$$\nabla(\nabla \cdot \boldsymbol{U}) \cdot \delta \boldsymbol{U} = \nabla \cdot ((\nabla \cdot \boldsymbol{U}) \delta \boldsymbol{U}) - (\nabla \cdot \boldsymbol{U})(\nabla \cdot \delta \boldsymbol{U}). \tag{7}$$

Hence, we obtain

$$\int_V \beta \nabla \cdot ((\nabla \cdot \boldsymbol{U}) \delta \boldsymbol{U}) \mathrm{d}V - \int_V \beta (\nabla \cdot \boldsymbol{U})(\nabla \cdot \delta \boldsymbol{U}) \mathrm{d}V = \int_V \rho \frac{\partial^2 \boldsymbol{U}}{\partial t^2} \cdot \delta \boldsymbol{U} \, \mathrm{d}V \tag{8}$$

and using the divergence theorem, with $\boldsymbol{n}$ the unit outward normal,

$$\int_S \beta (\nabla \cdot \boldsymbol{U}) \delta \boldsymbol{U} \cdot \boldsymbol{n} \mathrm{d}S - \int_V \beta (\nabla \cdot \boldsymbol{U})(\nabla \cdot \delta \boldsymbol{U}) \mathrm{d}V = \int_V \rho \frac{\partial^2 \boldsymbol{U}}{\partial t^2} \cdot \delta \boldsymbol{U} \, \mathrm{d}V. \tag{9}$$

Hence, the virtual work expression for the formulation

of a fluid element is given by

$$\int_V \beta(\nabla \cdot \boldsymbol{U})(\nabla \cdot \delta\boldsymbol{U})\mathrm{d}V + \int_V \rho \frac{\partial^2 \boldsymbol{U}}{\partial t^2} \cdot \delta\boldsymbol{U}\,\mathrm{d}V = -\int_S p\,\delta\boldsymbol{U} \cdot \boldsymbol{n}\,\mathrm{d}S. \tag{10}$$

This expression is employed frequently in transient analysis of fluid–structure systems. However, as pointed out by Hamdi et al. [25], the fact that the fluid is irrotational has been lost in this derivation. In other words, the solution of eq. (4) corresponds to an irrotational motion whereas the finite element solution obtained from eq. (10) does not necessarily satisfy irrotationality. Since the fluid motion physically must be irrotational, we follow Hamdi et al. and impose a penalty on rotations in the virtual work expression in eq. (10). Thus, the final virtual work principle used to predict the fluid motion is

$$\int_V \beta(\nabla \cdot \boldsymbol{U})(\nabla \cdot \delta\boldsymbol{U})\mathrm{d}V + \int_V \alpha(\nabla \times \boldsymbol{U}) \cdot (\nabla \times \delta\boldsymbol{U})\mathrm{d}V + \int_V \rho \frac{\partial^2 \boldsymbol{U}}{\partial t^2} \cdot \delta\boldsymbol{U}\,\mathrm{d}V = -\int_S p\,\delta\boldsymbol{U} \cdot \boldsymbol{n}\,\mathrm{d}S. \tag{11}$$

Note that as the speed of sound ($c = \sqrt{\beta/\rho}$) approaches infinity (i.e. $\beta \to \infty$), the operations in eq. (11) can be interpreted as minimizing the fluid's kinetic energy with penalties on motions involving compression and rotation.

Using the usual procedures the stiffness matrix for a fluid element is obtained by interpolating the displacement $\boldsymbol{U}$ in eq. (11). For planar motions the isoparametric finite element stiffness matrix is

$$\boldsymbol{K} = \boldsymbol{K}_{\mathrm{L}} + \boldsymbol{K}_{\mathrm{C}} = \int_V \beta \boldsymbol{V}^{\mathrm{T}}\boldsymbol{V}\mathrm{d}V + \int_V \alpha \boldsymbol{D}^{\mathrm{T}}\boldsymbol{D}\mathrm{d}V, \tag{12}$$

where

$$U_j = \sum_{i=1}^{N} h_i U_j^i, \quad j = 1, 2; \tag{13}$$

$$\boldsymbol{V} = [h_{1,1} \quad h_{1,2} \quad h_{2,1} \quad \dots \quad h_{N,2}], \tag{14}$$

$$\boldsymbol{D} = [h_{1,2} \quad -h_{1,1} \quad h_{2,2} \quad -h_{2,1} \quad \dots \quad -h_{N,1}], \tag{15}$$

$\frac{\beta}{12}$

4	3	-4	3	-2	-3	2	-3
3	4	-3	2	-3	-2	3	-4
-4	-3	4	-3	2	3	-2	3
3	2	-3	4	-3	-4	3	-2
-2	-3	2	-3	4	3	-4	3
-3	-2	3	-4	3	4	-3	2
2	3	-2	3	-4	-3	4	-3
-3	-4	3	-2	3	2	-3	4

$\frac{\alpha}{12}$

4	-3	2	3	-2	3	-4	-3
-3	4	-3	-4	3	-2	3	2
2	-3	4	3	-4	3	-2	-3
3	-4	3	4	-3	2	-3	-2
-2	3	-4	-3	4	-3	2	3
3	-2	3	2	-3	4	-3	-4
-4	3	-2	-3	2	-3	4	3
-3	2	-3	-2	3	-4	3	4

Fig. 1. $\boldsymbol{K}_{\mathrm{L}}$ (top) and $\boldsymbol{K}_{\mathrm{C}}$ for square four-node element of unit thickness with full integration.

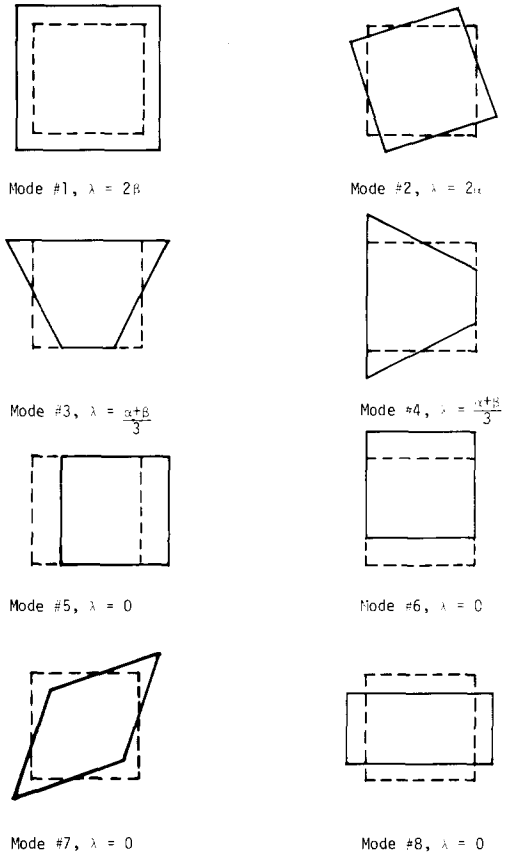

Fig. 2. Eigenvalues of four-node element including penalty function (full integration).

and the h_i are the interpolation functions [26].

Fig. 1 shows the matrices $\boldsymbol{K}_L$ and $\boldsymbol{K}_C$ for full integration of a four node plane element. The figure shows that the elements in the matrices are of the same order of magnitude when α is equal to β. In our finite element implementation α is always taken to be some multiple of β.

For a four-node fluid element $\boldsymbol{K}_L$ has exactly the same eigenvectors as $\boldsymbol{K}_C$ although the eigenvalues are different. This fact makes it simple to analyze a single four-node element with any penalty value, as revealed in fig. 2. Note that the penalty function only affects rotational modes.

4. Example problems

We examine four categories of fluid–structure interaction problems (see fig. 3). Category 1 consists of static problems, where the pressure is constant throughout the fluid. In category 2 we consider problems involving the natural frequencies of a fluid vibrating in a rigid cavity, and in category 3 we have fluids vibrating within flexible boundaries. Finally, category 4 involves flexible solid structures vibrating in a fluid. We will discuss solutions of problems in each of these categories.

4.1. Category one – Static problems

First we examine static fluid–structure interaction problems, since they are the simplest. Fig. 4 shows the tilted piston-container test case. By equating the applied force to the fluid pressure multiplied by the container's cross-sectional area we see that the correct displacement is

$$F = pA = \beta(\delta)AA/V,$$

$$\delta = FV/\beta A^2 = 0.025 \text{ m}.$$

Fig. 5 shows the mesh used to model the piston-container: 9-node elements for the fluid, 8-node elements for the solid, with the fluid constrained to move only tangent to the solid as shown. Fig. 5 also shows the finite element results for full integration without the penalty on fluid particle rotations, which are excellent. As shown in fig. 6, when we include the penalty term the results are not as accurate. A large number of elements are required to arrive at a good result using the penalty, and distorted elements do not perform as well as undistorted elements. (The second three meshes in fig. 6 produced more accurate results than the first three.) Since fluid particle motions are unimportant here, it is best to neglect the penalty on particle rotations in static analyses.

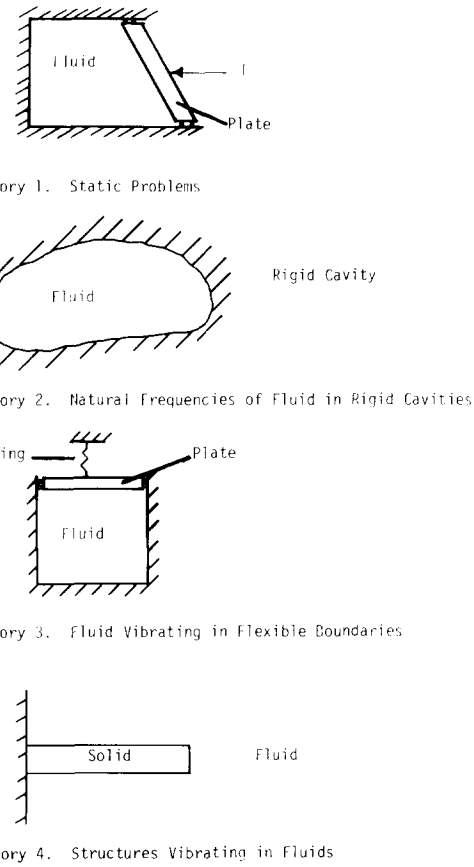

Fig. 3. Four categories of fluid–structure interaction problems.

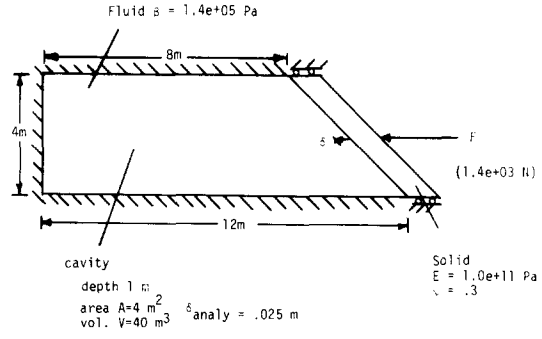

Fig. 4. Tilted piston-container test case.

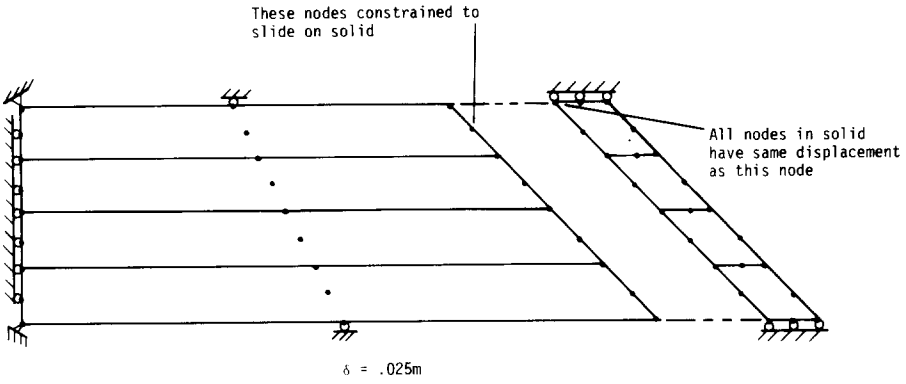

Fig. 5. Mesh and results for tilted piston-container problem without penalty.

4.2. Category two – Frequencies of fluid in rigid cavities

We calculated the resonant frequencies of several fluid-filled cavities using the formulation in eq. (11). Here we present results for a rigid box, a tall water column, and an infinite cylinder.

4.2.1. Rigid box

A compressible fluid vibrating in a rigid box is modeled as a two-dimensional problem. The solution of the wave equation for the first three frequencies and mode shapes yields (see fig. 7)

$$\omega_1 = 9132 \text{ rad/s}, \quad u_1 = 0, \quad u_2 = \sin\left(\frac{\pi x_2}{L}\right);$$

$$\omega_2 = 15\,220 \text{ rad/s}, \quad u_1 = \sin\left(\frac{\pi x_1}{l}\right), \quad u_2 = 0;$$

$$\omega_3 = 17\,749 \text{ rad/s}, \quad u_1 = \frac{1}{l}\sin\left(\frac{\pi x_1}{l}\right)\cos\left(\frac{\pi x_2}{L}\right),$$

$$u_2 = \frac{1}{L}\cos\left(\frac{\pi x_1}{l}\right)\sin\left(\frac{\pi x_2}{L}\right).$$

Note that the first two modes are simple plane waves, but the third mode is quite complex. Tables 1 and 2 show finite element results for various numbers of elements and assorted penalty parameters. In general, we should use $\alpha = 100\beta$ or 1000β to impose the irrotationality constraint.

4.2.2. Tall water column

Fig. 8 shows the "tall water column problem". This problem is similar to the rectangular box problem, except that the column is much higher than it is wide and has a free surface (pressure = 0). The solution to the wave equation for this problem gives

$$U_1 = A\lambda_1 \sin(\lambda ct)\cos(\lambda_2 x_2)\sin(\lambda_1 x_1),$$

$$U_2 = A\lambda_2 \sin(\lambda ct)\sin(\lambda_2 x_2)\cos(\lambda_1 x_1),$$

where

$$\lambda_1 = n\pi/l, \quad n = 0, 1, 2, 3\ldots,$$

$$\lambda_2 = m\pi/2L, \quad m = 1, 3, 5\ldots,$$

$$\omega = \lambda c = c\pi\left[\left(\frac{n}{l}\right)^2 + \left(\frac{m}{2L}\right)^2\right]^{1/2}.$$

Note that modes one through ten represent plane waves travelling the length of the column. Fig. 9 shows the mesh used to model the tall water column. Table 3 compares the analytical and finite element frequencies, which are in excellent agreement.

The tall water column problem allows us to examine the importance of the irrotationality parameter in the displacement-based analysis of fluid frequencies. Fig. 10 shows the first two modes calculated by the finite element method if the penalty on particle rotations is not included. Note that these modes do not represent surface waves, since gravity and sloshing were not included in the formulation. These displacement patterns represent unphysical (spurious) modes which occur at non-zero frequencies [23–25].

4.2.3. Infinite cylinder

To demonstrate the formulation's ability to handle non-plane waves we analyzed a rigid, infinitely long cylinder filled with compressible fluid. The transverse vibration frequencies are [27]

$$p = \begin{matrix}\cos\\ \sin\end{matrix}(m\phi)J_m\left(\frac{\omega r}{c}\right)e^{-i\omega t},$$

$$\omega = \pi\alpha_{mn}c/a,$$

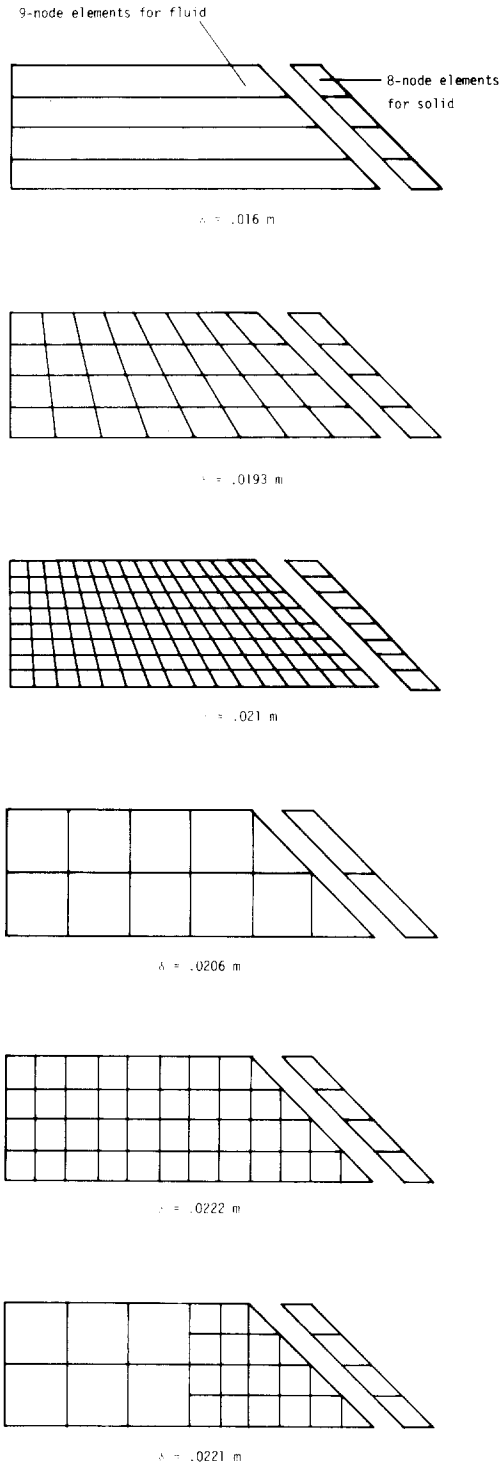

Fig. 6. Meshes and results for tilted piston-container problem with penalty.

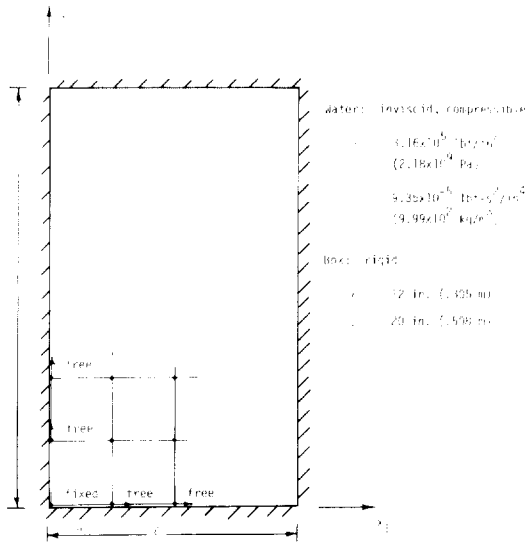

Fig. 7. Constants for calculating resonant frequencies of box.

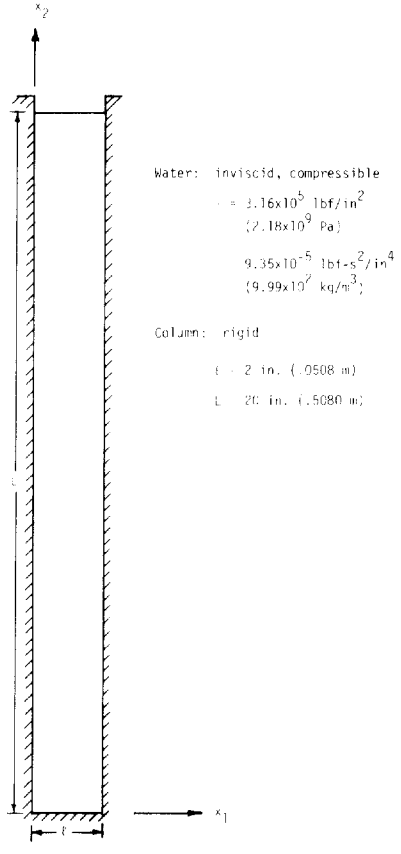

Fig. 8. Tall water column problem.

Table 1
Analytical and finite element solutions for natural frequencies of fluid in rigid rectangular box (using four-node finite elements with full integration)

	$\alpha = 10\beta$	$\alpha = 1\beta$	$\alpha = 0.1\beta$	$\alpha = 0$
First mode (9132 rad/s)				
4 elem	10070	10070	8409	6000
16 elem	9368	9368	6277	2634
64 elem	9191	9191	5776	1271
256 elem	9147	9147	5653	630
Second mode (15220 rad/s)				
4 elem	16780	16780	10070	10070
16 elem	15610	15610	9368	4913
64 elem	15320	15320	8192	2278
256 elem	15240	15240	7684	1116
Third mode (17749 rad/s)				
4 elem	65860	19750	14630	10070
16 elem	19850	18210	10390	6910
64 elem	18270	17860	9191	3081
256 elem	17880	17780	9147	1496

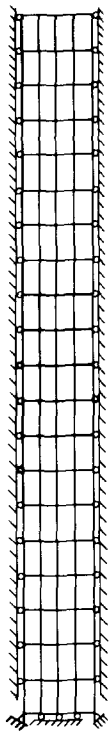

Fig. 9. Finite element mesh used for tall water column.

Table 2
Analytical and finite element solutions for natural frequencies of fluid in rigid rectangular box (using eight-node elements with full integration)

	$\alpha = 1000\beta$	$\alpha = 100\beta$	$\alpha = 10\beta$	$\alpha = 1\beta$	$\alpha = 0.1\beta$
First mode (9132 rad/s)					
1 elem	9192	9192	9192	9192	5984
4 elem	9166	9166	9166	9166	5705
16 elem	9134	9134	9134	9134	5619
Second mode (15220 rad/s)					
1 elem	15320	15320	15320	15320	9192
4 elem	15280	15280	15280	15280	7948
16 elem	15220	15220	15220	15220	7596
Third mode (17749 rad/s)					
1 elem	157000	52450	23700	18330	15320
4 elem	18380	18380	18040	17850	9166
16 elem	17980	17850	17770	17750	9134

Table 3
Analytical and finite element solutions to natural frequencies of tall water column with full integration

Mode #	Analytical solution (rad/s)	Finite element solution (rad/s)
1	4566	4567
2	13698	13730
3	22830	22890

where

ϕ = polar angle,
r = radial coordinate,
a = cylinder radius,
J_m = Bessel function of the first kind of order m,
α_{mn} = a solution to $\mathrm{d}J_m(\pi\alpha)/\mathrm{d}\alpha = 0$.

For a cylinder filled with water (speed of sound $c =$ 58 135 in/s, radius $a = 5$ in), we find that

$\omega_{1,2} = 21\,400$ rad/s,

$\omega_{3,4} = 35\,500$ rad/s,

$\omega_{5,6} = 44\,600$ rad/s,

where each is a double eigenvalue (corresponding to the cosine and sine modes of p).

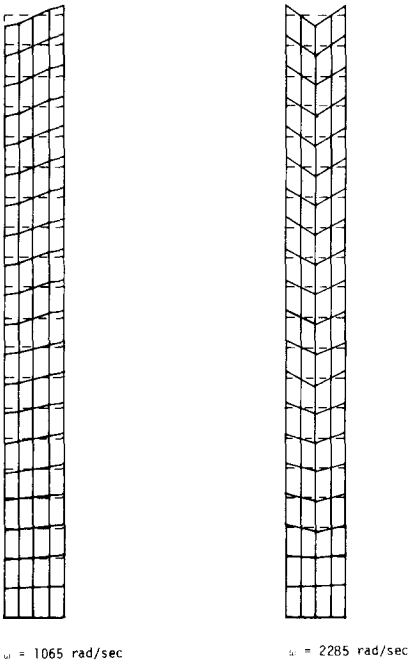

Fig. 10. Spurious modes for tall water column without penalty.

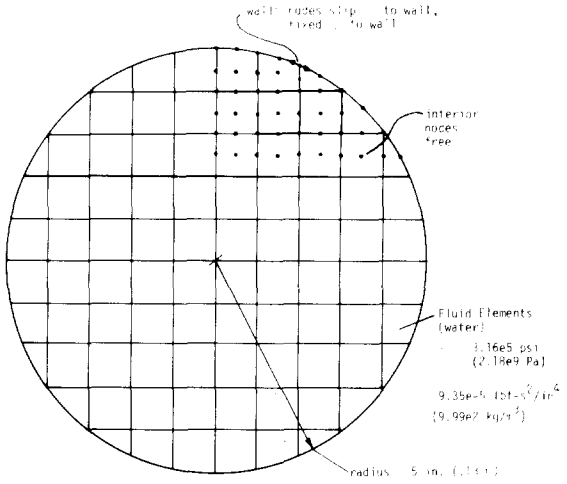

Fig. 11. Mesh used for infinite cylinder problem.

Fig. 11 shows the finite element mesh used. Note that it includes distorted elements, and that the waves will move at various angles to the sides of the elements. Table 4 compares finite element and analytical frequencies. The finite element solution predicts the first 6 modes with good accuracy.

4.3. Category three – Frequencies of fluids in flexible boundaries

To study a fluid–structure interaction problem which has an analytical solution, we chose the piston/container/spring arrangement shown in fig. 12. To solve this problem analytically requires that we consider the mass-spring system separately from the fluid.

The plate is infinitely rigid and therefore imposes a displacement on the top surface of the fluid at some (as yet) unknown frequency

$$u_2 = a\sin(\omega t) \quad \text{at } x_2 = L.$$

Table 4
Analytical and finite element solutions to infinite cylinder problem with full integration (9-node elements)

Mode #	Analytical value	Finite element result
1	2.14e4	2.14e4
2	2.14e4	2.15e4
3	3.55e4	3.56e4
4	3.55e4	3.57e4
5	4.45e4	4.47e4
6	4.45e4	4.92e4

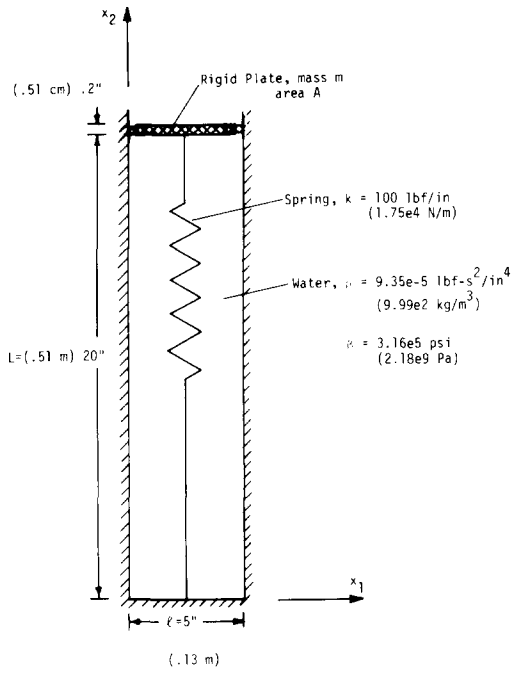

Fig. 12. Piston-container problem.

Solving the wave equation for the fluid, we find that the pressure distribution in the fluid must be

$$p = \frac{-a\rho\omega c}{\sin(\omega L/c)} \cos\left(\frac{\omega x_2}{c}\right) \sin(\omega t).$$

At the plate surface the pressure exerted by the fluid is

$$p|_{x_2=L} = -a\rho\omega c \cot\left(\frac{\omega L}{c}\right) \sin(\omega t).$$

This pressure acts on the mass-spring system like an equivalent spring whose stiffness depends on frequency

$$k_{\text{equivalent}} = \rho\omega cA \cot(\omega L/c)$$

Hence the frequency of the mass-spring–equivalent spring system is

$$\omega = \sqrt{[k + \rho\omega cA \cot(\omega L/c)]/m}.$$

Non-dimensionalizing this equation gives

$$\xi = \sqrt{[m_k + m_f \xi \cot(\xi)]/m}$$

where

$$\xi = \omega L/c,$$

$$m_f = \rho AL,$$

$$m_k = kL^2/c^2.$$

Choosing the values for the constants given in fig. 12, the relation between the mass of the plate and the frequency of the entire system shown in fig. 13 is obtained.

Fig. 14 shows the finite element model used to solve this problem. Constraint equations were employed to model the rigid plate, and two 8-node solid and four 9-node fluid elements were used. Table 5 presents the analytical and finite element results, which compare favorably.

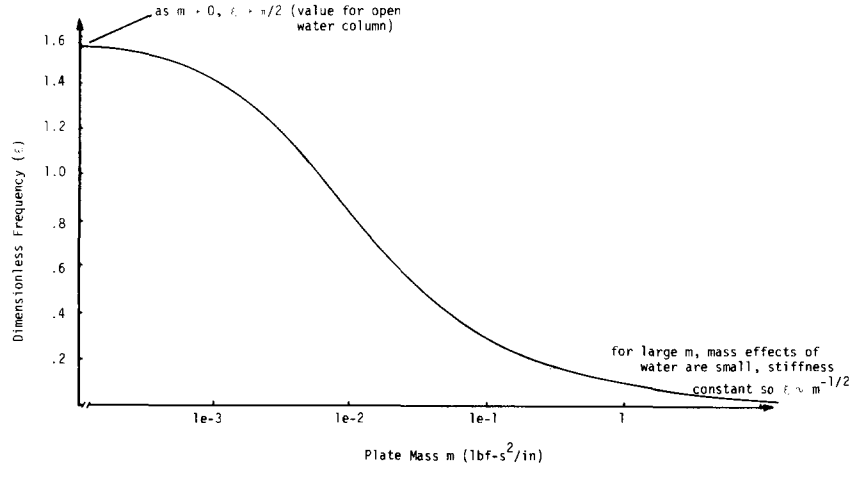

Fig. 13. Dimensionless frequency ξ vs. plate mass m for piston-container problem.

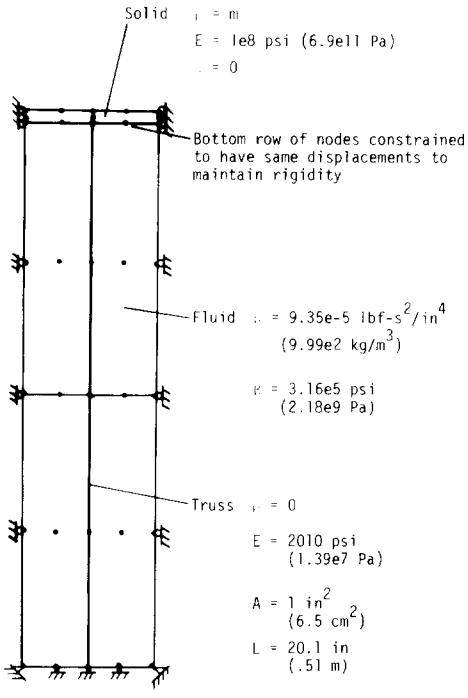

Fig. 14. Finite element model of piston-container problem.

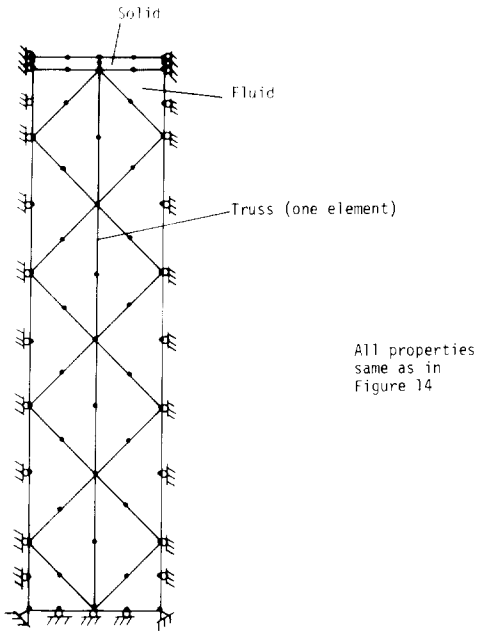

Fig. 15. Alternate finite element model of piston-container problem.

To check the effect of fluid element orientation on accuracy, the mesh in fig. 15 was also used. Here we use four 9-node elements and ten spacially isotropic 6-node triangular elements. The results are the same as for the original mesh.

4.4. *Category four–Frequencies of flexible structures in fluids*

Ultimately, we hope to be able to solve general fluid–structure interaction problems (see fig. 3d). Initially, however, we would like to solve what would appear to be a fairly simple fluid–structure resonance problem.

Table 5
Analytical and finite element solutions to piston-container problem with full integration

Piston mass	Frequency in vacuum	Analytical frequency in water	Finite element frequency in water
1.0	10	281	281
0.1	31.6	876	876
0.01	100	2441	2441
0.001	316	4130	4131

Fig. 16 shows the problem considered: a solid ellipse is suspended on a spring and immersed in water. For low vibration frequencies ($L\omega/c \ll 1$) fluid density changes will be negligible, the fluid acts as incompressible, and we may use the results of incompressible potential theory to find the "added mass" due to the fluid and hence find the resonant frequency of this system.

Note that this is a nearly incompressible fluid flow problem which we want to consider as a limiting case of compressible fluid motion, whereas the problems in categories 1 to 3 were truly acoustic problems.

The natural frequency of the ellipse-spring system in vacuum is 31.6 rad/s. When the ellipse vibrates in the fluid, it must move an additional mass of fluid known as the "added mass" m', which from incompressible potential theory is known to be [28]

$$m' = \rho_f \pi a^2.$$

The natural frequency of the mass-spring system in water is thus

$$\omega = \sqrt{k/(m + m')} = 28.2 \text{ rad/s},$$

which represents only an 11% decrease in frequency.

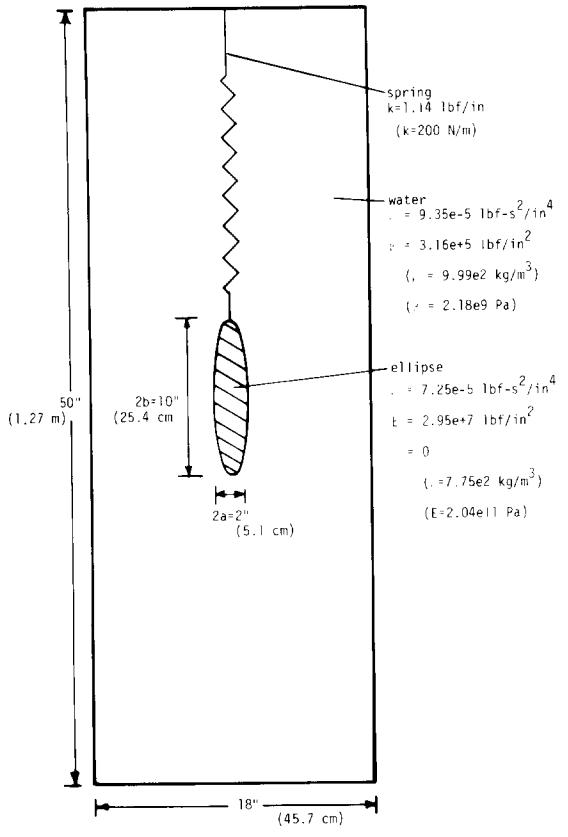

Fig. 16. Ellipse-on-spring problem.

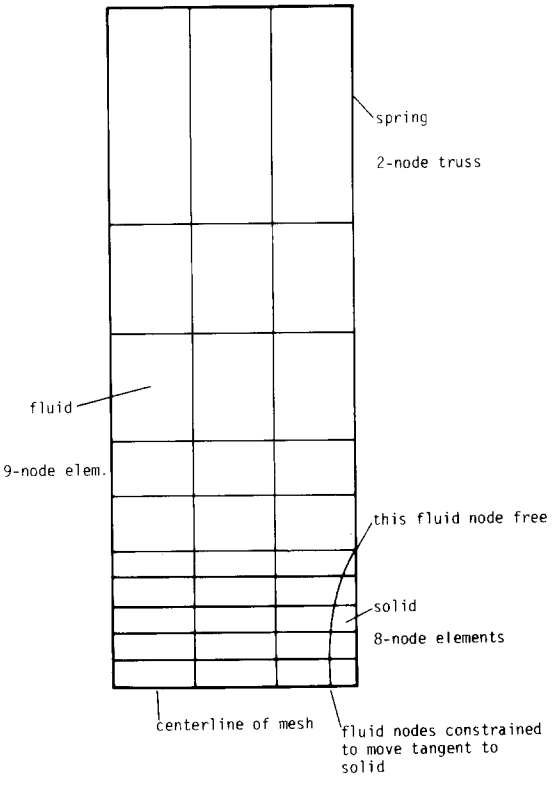

Fig. 17. First mesh used to model ellipse-on-spring.

4.4.1. Finite element models and results

Fig. 17 shows the upper half of a finite element mesh (mesh #1) used to model the ellipse-on-spring problem. This mesh uses nine-node fluid elements for the water, eight-node solid elements for the ellipse, and a 2-node truss to model the spring. At the surface of the ellipse, fluid and solid nodes lie on top of each other initially, and the fluid nodes are forced to move along the ellipse by constraint equations. With full integration, the finite element analysis gives a natural frequency for the system $\omega = 3668$ rad/s, which is within 1% of the first frequency of the fluid alone in the 50 in (1.27 m) long box.

Results from the static cases in section 4.1 implied that the displacement/penalty element converges very slowly, and is sensitive to distortion. Therefore, we attempted to model the ellipse-on-spring problem with a much finer mesh. Model #2 (see fig. 18) contains approximately ten times as many elements as model #1, and the elements are undistorted. Again we used

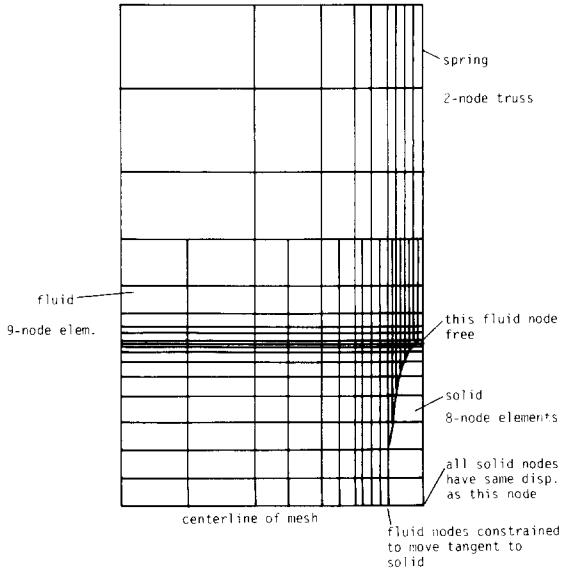

Fig. 18. Second mesh used to model ellipse-on-spring.

9-node fluid elements, 8-node solid elements, and a 2-node truss, but to reduce the number of degrees of freedom in the model the box is only 30 in (0.76 m) long and all of the ellipse nodes have the same displacements. As before, however, this second model gave a natural frequency ($\omega \approx 6126$ rad/s) which corresponds to the first frequency of the fluid alone in the new 30 in (0.76 m) long box.

One approach used when a finite element mesh is too stiff is underintegration. With two point integration the first model of the ellipse-on-spring problem yields an answer of 26.0 rad/s. This solution is the first eigenvalue of the matrix system, i.e. there are no zero frequencies below this one. However this answer is about 8% too low, and the change in frequency between vacuum and water is only 11 percent. Fig. 19 shows the resulting mode shape.

With full integration, we seek the solution to the problem governed by the known differential operator. Using underintegration we actually work with another, unknown, differential operator. Since we do not know the differential operator corresponding to the analysis of the ellipse, we decided not to investigate underintegration further until we better understand the full integration results.

4.4.2. Analysis of a dipole velocity field

Whenever any solid moves through an incompressible fluid with a steady velocity, its velocity field is that of a dipole (or doublet) to first order [29]. A dipole is the velocity field that a cylinder produces when it moves through an incompressible fluid. Denoting ϕ as the velocity potential, and ψ as the stream function, we have [28]

$$\phi = -Ur_0^2 x_1/(x_1^2 + x_2^2),$$

$$\psi = -Ur_0^2 x_2/(x_1^2 + x_2^2),$$

where

U = velocity of cylinder,
r_0 = cylinder radius,
x_1 = distance from cylinder center along axis of motion,
x_2 = distance from cylinder center perpendicular to axis of motion,

To calculate the fluid velocities we use $\boldsymbol{V} = \nabla\phi$ so that

$$V_1 = -Ur_0^2(x_2^2 - x_1^2)/(x_1^2 + x_2^2)^2,$$

$$V_2 = Ur_0^2(2x_1x_2)/(x_1^2 + x_2^2)^2.$$

For our discussion we note that the flow field caused by a cylinder as it moves through the fluid is both incompressible and irrotational

$$\text{incompressible:} \quad \nabla \cdot \boldsymbol{V} = \nabla^2\phi = 0,$$

$$\text{irrotational:} \quad \nabla \times \boldsymbol{V} = \nabla \times \nabla\phi = 0.$$

Hence, if we use the variational indicator for this exact incompressible flow solution, we obtain the virtual work expression

$$\int_V \beta(\nabla \cdot \delta\boldsymbol{U})(\nabla \cdot \boldsymbol{U})\,dV + \int_V \alpha(\nabla \times \delta\boldsymbol{U}) \cdot (\nabla \times \boldsymbol{U})\,dV + \int_V \frac{\partial^2 \boldsymbol{U}}{\partial t^2} \cdot \delta\boldsymbol{U}\,dV = 0 + 0 + \int_V \frac{\partial^2 \boldsymbol{U}}{\partial t^2} \cdot \delta\boldsymbol{U}\,dV,$$

and the solution of the problem corresponds to minimizing the kinetic energy of the fluid flow.

For finite element analysis, we hope to approximate the exact flow patterns closely. With the penalty/displacement element the first two terms of the variational indicator act as penalties on compression and rotation, but for an accurate solution they must remain small with respect to the kinetic energy term. Fig. 20 shows the exact flow streamlines that occur when a cylinder moves through water. The cylinder radius is the

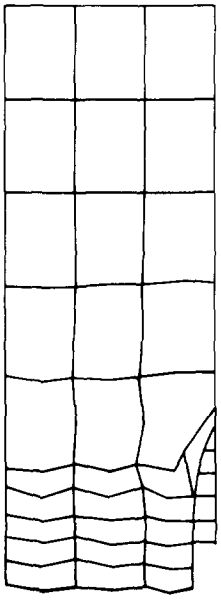

Fig. 19. First mode of mesh #1 with 2-point integration.

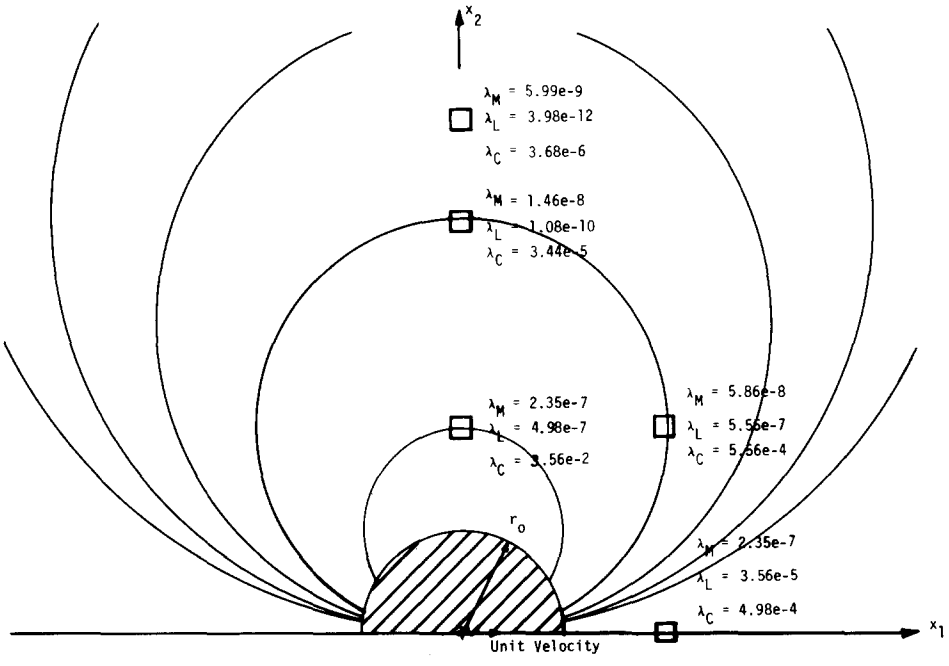

Fig. 20. Finite elements superimposed on dipole streamlines. $r_0 = 1$ in (2.54 cm); $\beta = 3.16e5$ lbf/in^2 (2.18e9 Pa); $\alpha = 1000\beta$; $\rho = 9.35e-5$ lbf s^2/in^4 (9.99e2 kg/m^3); λ_M = energy in mass $\equiv \dot{\boldsymbol{U}}^T \boldsymbol{M} \dot{\boldsymbol{U}}$; λ_L = energy in compression $\equiv \boldsymbol{U}^T \boldsymbol{K}_L \boldsymbol{U}$; λ_C = energy in rotation penalty $\equiv \boldsymbol{U}^T \boldsymbol{K}_C \boldsymbol{U}$; $\boldsymbol{U} = \dot{\boldsymbol{U}}/30$ (i.e. $\omega = 30$); energy in in-lbf (0.113 Nm).

half-width of the ellipse, and the ratio of velocities to displacements is typical of what could occur in an oscillatory flow with $\omega = 30$ (approximately the ellipse frequency). Fig. 20 also shows (to scale) several 9-node finite elements placed "in" the flow. By analytically calculating the velocities that should occur at each node of an element, and applying these velocities to the nodes, we calculated the energies in the rotation, compression, and mass terms of the variational indicator. With this correct velocity distribution we should get approximately the correct energy distribution if we hope to obtain accurate mode shapes and frequencies from a finite element model. As shown in fig. 20, the penalty and compression terms can be large relative to the mass term, although they should be small. λ_C dominates but must be included, as discussed previously. In addition, λ_L is sometimes much larger than λ_M. This indicates that penalty/displacement-based elements cannot correctly model the velocity field produced by a cylinder in steady flow.

Hence, we should not expect to find the resonant frequencies of the ellipse-spring fluid–structure system accurately with displacement-based finite elements.

5. Summary and conclusions

We draw four basic conclusions from this research:

(1) For static analysis, displacement-based fluid elements may be used reliably without a penalty. In this case, the actual motion of the fluid particles is unimportant. Displacement-based elements capture volume changes accurately and therefore give excellent results without a penalty on rotations.

(2) Displacement-based fluid elements with a penalty applied on rotations may be used reliably for all problems involving resonant frequency analysis of arbitrarily shaped cavities. For the cavities tested, we obtained frequencies which are in excellent agreement with analytically calculated frequencies. Problems involving plane compression waves in rigid boxes or tall columns gave excellent results. The analysis of a compressible fluid in an infinite cylinder which required the circular compression waves to travel through rectangular finite elements also produced good results.

(3) Using the displacement-based fluid elements with a penalty applied on rotations, it appears that we can solve problems involving resonant frequency analysis of

fluids contained within flexible boundaries. A simple fluid–structure problem involving a spring-mounted plate on top of a column of compressible water produced accurate results over a wide range of frequencies.

(4) We cannot directly (ie. without underintegration or special modeling procedures [30]) solve problems involving the natural frequencies of structures in fluids using the displacement/penalty fluid finite element. In these problems the fluid behaves almost incompressibly, whereas in categories 1 to 3 the fluid is truly acoustic. The reason why the formulation is not able to model the fluid–structure motion was identified by studying the formulation applied to a dipole field. If a solid object moves through a fluid, its velocity field is approximately a dipole field (the velocity field produced by a cylinder moving through an incompressible fluid). When we attempt to model a dipole field with our displacement/penalty element, we find that the stiffness energy (although it should be zero) is much greater than the kinetic energy. Since the correct velocity field does not produce an accurate distribution of the total energy among the compression, rotation, and mass terms, it appears that we cannot model these fluid–structure interaction problems successfully.

The displacement and displacement/penalty fluid finite elements can be used for many truly acoustic problems of engineering concern with good results. However, when considering fluid motion that is almost incompressible this element can not be applied with confidence, and more work is required to clarify proper modeling with the element in these areas.

Acknowledgements

We are grateful for the financial support of ADINA Engineering AB, Sweden, and the Forschungszentrum GKSS, West Germany for this work. We also thank G. Larsson, ADINA Engineering, and T. Belytschko, Northwestern University, for their comments on this research.

References

[1] O.C. Zienkiewicz and P. Bettess, Fluid–structure dynamic interaction and wave forces. An introduction to numerical treatment, Internat. J. Numer. Meth. Engrg. 13 (1978) 1–16.

[2] T.B. Belytschko, Methods and programs for analysis of fluid–structure systems, Nucl. Engrg. Des. 42 (1977) 41–52.

[3] T.B. Belytschko, Fluid–structure interaction, Computers and Structures 12 (1980) 459–469.

[4] O.C. Zienkiewicz and R.E. Newton, Coupled vibrations of a structure submerged in a compressible fluid, Symposium on Finite Element Techniques, Stuttgart, 1969.

[5] A. Craggs, The transient response of a coupled plate-acoustic system using plate and acoustic finite elements, J. of Sound and Vibration 15 (1971) 509–528.

[6] W.C. Muller, Simplified analysis of linear fluid–structure interaction, Internat. J. Numer. Meth. Engrg. 17 (1981) 113–121.

[7] H. Morand and R. Ohayon, Substructure variational analysis of coupled fluid–structure systems. Finite elment results, Internat. J. Numer. Meth. Engrg. 14 (1979) 741–755.

[8] M. Petyt and S.P. Lim, Finite element analysis of the noise inside a mechanically excited cylinder, Internat. J. Numer. Meth. Engrg. 13 (1978) 109–122.

[9] T.B. Belytschko and J.M. Kennedy, A fluid–structure finitê element method for the analysis of reactor safety problems, Nucl. Engrg. Des. 38 (1976) 71–81.

[10] T.B. Belytschko and J.M. Kennedy, Computer models for subassembly simulation, Nucl. Engrg. Des. 49 (1978) 17–38.

[11] T. Belytschko and U. Schumann, Fluid–structure interactions in light water reactor systems, Nucl. Engrg. Des. 60 (1980) 173–195.

[12] T. Belytschko and R. Mullen, Two dimensional fluid–structure impact computations with regularization, Computer Meth. Appl. Mech. Engrg. 27 (1981) 139–154.

[13] T.B. Belytschko and D.P. Flanagan, A uniform strain hexahedron and quadrilateral with orthogonal hourglass control, Internat. J. Numer. Meth. Engrg. 17 (1981) 676–706.

[14] K.J. Bathe and W. Hahn, On transient analysis of fluid–structure systems, Computers and Structures 10 (1978) 383–391.

[15] G. Larsson and P. Svenkvist, Experiences using the ADINA fluid element for large displacement analysis, Proceedings of the ADINA Conference, August 1979, pp. 383–406.

[16] G.M.L. Gladwell and G. Zimmerman, On energy and complementary energy formulations of acoustic and structural vibration problems, J. of Sound and Vibration 3 (1966) 233–241.

[17] G.M. Gladwell, A variational formulation of damped acousto-structural vibration problems, J. of Sound and Vibration 4 (1966) 172–186.

[18] A.K. Chopra, E.L. Wilson and I. Farhoomand, Earthquake analysis of reservoir-dam systems, Proceedings of the 4th World Conference on Earthquake Engineering, Santiago, Chile, 1969.

[19] E.L. Wilson, Chap. 10 of: Finite Elements in Geomechanics, Ed.: Gudehus (John Wiley and Sons, New York, 1977), paper at the International Symposium of Numerical Methods in Soil Mechanics and Rock Mechanics, Karlsruhe, September 1975.

[20] D. Shantaram, D.R.J. Owen and O.C. Zienkiewicz, Dy-

namic transient behaviour of two- and three-dimensional structures including plasticity, large deformation effects, and fluid interaction, Earthq. Engrg. Struct. Dyn. 4 (1976) 561–578.

[21] T.A. Shugar and M.G. Katona, Development of finite element head injury model, J. Engrg. Mech. Div. ASCE (June 1975) 223–239.

[22] T.B. Khalil and R.P. Hubbard, Parametric study of head response by finite element modelling. J. of Biomechanics 10 (1977) 119–132.

[23] L. Kiefling and G.C. Feng, Fluid structure finite element vibration analysis, AIAA Journal 14 (1976) 199–1203.

[24] N. Akkas, H. Akay and C. Yilmaz, Applicability of general purpose finite element programs in solid–fluid interaction problems, Computers and Structures 10 (1978) 773–783.

[25] M.A. Hamdi, Y. Ousset and G. Verchery, A displacement method for the analysis of vibrations of coupled fluid–structure systems, Internat. J. Numer. Meths. Engrg. 13 (1978) 139–150.

[26] K.J. Bathe, Finite Element Procedures in Engineering Analysis (Prentice-Hall, Inc., Englewood Cliffs, NJ, 1982).

[27] P.M. Morse, Vibration and Sound, Published by the American Institute of Physics for the Acoustical Society of America (1976).

[28] T. Sarpkaya and M. Isaacson, Mechanics of Wave Forces on Offshore Structures (Van Nostrand Reinhold Company, New York, 1981).

[29] G.K. Batchelor, An Introduction to Fluid Dynamics (Cambridge University Press, New York, 1981).

[30] J. Sundqvist, An application of ADINA to the solution of fluid-structure interaction problems, Computers and Structures 17 (5/6) (1983) 793–807.